SoftwareX 12 (2020) 100574

Contents lists available at ScienceDirect

SoftwareX

journal homepage: www.elsevier.com/locate/softx

Original software publication

MULTIFRAC: An ImageJ plugin for multiscale characterization of 2D and 3D stack images

Iván .G. Torre [a,b,*], Richard J. Heck [c], A.M. Tarquis [d,e,f]

[a] Vicomtech Foundation, Basque Research and Technology Alliance (BRTA), San Sebastian, Spain
[b] Complexity and Quantitative Linguistics Lab, LARCA Research Group, Departament de Ciències de la Computació, Universitat Politècnica de Catalunya, Barcelona, Spain
[c] School of Environmental Sciences, Ontario Agricultural College, University of Guelph, Canada
[d] Complex Systems Group (GSC), Universidad Politécnica de Madrid (UPM), Madrid, Spain
[e] CEIGRAM, ETSIAAB, Universidad Politécnica de Madrid (UPM), Madrid, Spain
[f] Department of Applied Mathematics, ETSIAAB, Universidad Politécnica de Madrid (UPM), Madrid, Spain

ARTICLE INFO

Article history:
Received 12 May 2020
Received in revised form 28 July 2020
Accepted 28 July 2020

Keywords:
Multifractal
Lacunarity
Configuration entropy
ImageJ

ABSTRACT

MULTIFRAC is an ImageJ plugin that addresses, through a user-friendly interface, the characterization and multiscaling analysis of 2D and 3D binary and gray images. It is notably recommended for the study of complex void structure and scaling behavior in soil science as well as for the analysis of self-similar patterns in any segmented phase. The main features of MULTIFRAC include multifractal analysis implementing box counting and gliding box methodologies, fractal dimension estimation, lacunarity characterization, characteristic length and configuration entropy analysis. It has been extensively tested with real and synthetic CT-images and the conclusions were published in high impact factor journals. In this paper, we detail and reference the algorithms implemented, describe its features and give some illustrative examples.

Code metadata

Current code version	v1.0
Permanent link to repository used for this code version	https://github.com/ElsevierSoftwareX/SOFTX_2020_210
Code Ocean compute capsule	-
Legal Code License	GNU General Public License v3.0
Code versioning system used	Git
Software code languages, tools, and services used	Java, ImageJ2, Maven
Compilation requirements, operating environments & dependencies	Openjdk 8, Maven and ImageJ2 libraries
If available Link to developer documentation/manual	https://imagej.net/Multifrac
Support email for questions	igonzalez@vicomtech.org

Software metadata

Current software version	1.0
Permanent link to executables of this version	https://sites.imagej.net/Multifrac/plugins/
Legal Software License	GNU General Public License v3.0
Computing platforms/Operating Systems	Linux, OS X, Microsoft Windows
Installation requirements & dependencies	ImageJ2/FIJI
If available, link to user manual - if formally published include a reference to the publication in the reference list	https://imagej.net/Multifrac
Support email for questions	igonzalez@vicomtech.org

* Corresponding author at: Vicomtech Foundation, Basque Research and Technology Alliance (BRTA), San Sebastian, Spain.
E-mail address: igonzalez@vicomtech.org (I. Torre).

https://doi.org/10.1016/j.softx.2020.100574

1. Motivation and significance

Computational image analysis has increasingly been applied to many engineering and science fields in recent decades by the hand of technological and computational advances. Particularly, imaging techniques such as X-ray computed tomography (CT) revealed new perspectives in the analysis of hidden complex structures in natural systems, improving new ways of approaching the understanding of its underlying dynamics [1]. This is the case of soil science, where CT-scan analysis has opened a new paradigm to quantitatively characterize soil heterogeneity, which in the end, holds the key to understanding what are the physical, chemical and biological processes that take place in the soil [2,3].

Statistical physics provides a fruitful framework for relating individual contributions to macroscopic properties at higher system scales [4–6] and particularly, fractal and multifractal analysis deal with scaling behavior across scales. Moreover, the understanding of complex patterns that emerge across scales in many natural systems are addressed by other measures including multifractal analysis, lacunarity and configuration entropy. Those methodologies have been successfully applied to the analysis of CT-scan images to catalyze research in several scientific areas including characterization of human vessels [7], texture classification [8], cancer detection and tracing [9], neurodegenerative pathological detection [10], landsat imagery analysis [11] and quantification of complex structure in soil science [12–18] among others. However, the lack of an efficient, user-friendly and reliable implementation of multifractal analysis algorithms, could constitute a challenge for experimental research groups with less know-how in applied mathematics and computational physics. Although there are some available software options [19,20], they have not implemented all possible algorithms or they are not fully documented. MULTIFRAC aims to solve this issue by providing a user-friendly, open access, reliable tool for research on complex patterns in 2D and 3D images, which will be decidedly useful to several research groups among the world.

MULTIFRAC is designed to be a fully integrated ImageJ plugin [21], which, is an image processing tool with graphical user interface (GUI) extensively used through a wide range of scientific research areas. The ImageJ open architecture, which supports upgrades though JAVA plugin implementation, has made this software a very popular option to carry out research analysis on many kinds of images. MULTIFRAC has been successfully and extensively tested with real data and the results published in high impact, peer-reviewed scientific journals [12–14]. Algorithms implemented in MULTIFRAC for scaling and complexity analysis are fully documented through the following subsections.

1.1. Fractal dimension analysis on binary images

Fractal dimension (FD) analysis provides an index of complexity to objects that do not follow euclidean dimensions, assigning them a fractional dimension. This is the case of mathematical objects such as Cantor set, Sierpinski carpet or Mandelbrot set, but the same happens in natural phenomena, including frost crystals [22], coastlines [23] and craters [24]. Fractal dimension estimation is computed as follows: a 2D or 3D binary image of length size L is covered with non-overlapping boxes/cubes of length size $l < L$, being $N(l)$ the number of boxes/cubes required at each scale l to cover the mass area (black or white). Then FD is the scaling exponent between empty and non-empty boxes over scales [22]:

$$FD = \lim_{l \to 0} \frac{\log N(l)}{\log l} \tag{1}$$

1.2. Multifractal analysis of 2D/3D images using box counting and gliding box

Multifractal analysis needs to prior partition the space of study at different scales $l < L$, and given a 2D/3D gray image with length side L there are two main different strategies to do this [25]: (i) box counting method (BC) and (ii) gliding box method (GB), also called sliding box. BC grids the surface/space of analysis with non-overlapping boxes/cubes, and hence the number of boxes at each scale will be $n^*(l) \sim (L/l)^D$ where $D = 2$ for 2D images and $D = 3$ for 3D images. Meanwhile, GB starts placing a box/cube in the upper left-hand corner of the image and then it is translated by one pixel in one direction each time until it reaches the opposite extreme of the image, at which point it has explored every one of its possible positions where it will have sampled $n^*(l) = (L - l + 1)^D$ boxes/cubes. Although computationally much more expensive, GB provide less noisy and more stable results than BC. Regarding the method selected, for each box i it is calculated a probability mass function:

$$P_i(l) = \frac{m_i(l)}{\sum_i^{n^*(l)} m_i} \tag{2}$$

where $m_i(l)$ is computed as the sum of all pixels within box i, and hence $P_i(l)$ is the dimensionless mass contribution of box i at size l to the total, being $\sum_{m=1}^{N} P(m, l) = 1$. Multifractal analysis decomposes data into subsets characterized by multifractal spectrum and partition function with Holder exponent values that quantify local regularity behaviors [26]. The partition function $\chi(q, l)$ for the moments of order q of the probability mass distribution is defined as follows [27]:

$$\chi(q, l) = \sum_{m=0}^{N} P_i(l) \tag{3}$$

where q is a real number that represents the order of the mass distribution. When the phenomena under study follows a multifractal pattern, the partition function $\chi(q, l)$ scales with l following a power law function, so [28,29]:

$$\chi(q, l) \sim l^{\tau(q)} \tag{4}$$

where $\tau(q)$ is a probabilistic measure known as the cumulant generating function of order q [28] which can therefore be obtained as:

$$\tau(q) \sim \lim_{l \to 0} \frac{log\, \chi(q, l)}{log(l)} \tag{5}$$

Generalized dimensions D_q, characterize the mass density distortion over scales representing the multifractality robustness of the system. The more constant D_q is, the weaker the multifractality is. They are derived from $\tau(q)$ as follows:

$$D_q = \frac{\tau(q)}{(q - 1)} \tag{6}$$

where D_1 is evaluated using l'Hopital's Rule:

$$D_1 = \lim_{l \to 0} \frac{\sum_i P_i(l) \log P_i(l)}{\log l} \tag{7}$$

D_0 is called the capacity dimension, D_1 is referred to as the information dimension and it is related to Shannon's entropy, capturing how even the data density is, with higher values of D_1 meaning a more uniform density and finally, D_2 is referred as the correlation dimension which measures how scattered is the data, with increasing compactness for increasing values of D_2 [30]. Then, multifractal spectrum $f(\alpha)$ and local Hölder exponents, $\alpha(q)$, are derived from the cumulant generating functions as follows:

$$f(\alpha) = q\alpha - \tau\alpha = \frac{d\tau}{dq} \tag{8}$$

where the spread of α values indicates the scaling variety presents in the sample and $f(\alpha)$ values represents the strength of each α contribution [30].

1.3. Lacunarity

Lacunarity is a deviation measure of the gap sizes distribution in a given geometric object when doing translational invariance. In objects with low lacunarity values, different regions across the image are similar to each other, while in contrast, in a high lacunarity object, different regions may be very dissimilar and cannot be made to coincide by simple translation. This characterization is highly scale dependent and objects heterogeneous at small scales, can be homogeneous when examined at larger scales or vice versa [31].

Lacunarity analysis is implemented here using GB method, where mass m of box i at scale l is computed as the sum of all pixels contained in it. Following this procedure probability mass distribution $P(m, l)$ is the probability of obtaining a particular mass m in the image for a window size l being $\sum_{m=1}^{N} P(m, l) = 1$, where N is the number of possible mass values in the box of size l. Lacunarity is then defined as [32]:

$$\Lambda(l) = \frac{M^{(2)}(l)}{(M^{(1)}(l))^2} \tag{9}$$

where $M^{(1)}$ and $M^{(2)}$ are the first and second moments of mass distribution $P(m, l)$:

$$\begin{aligned} M^{(1)}(l) &= \sum_{m=1}^{N} mP(m, l) \\ M^{(2)}(l) &= \sum_{m=1}^{N} m^2 P(m, l) \end{aligned} \tag{10}$$

1.4. Configuration entropy and characteristic length

Configuration entropy is the portion of entropy in a system that is due to the location of its constituent elements. It is related to system disorder and we implement here configuration entropy analysis using GB method: covering the image with $n^*(l)$ boxes of size l, the probability of having $n_m(l)$ boxes with mass m is $p_m(l) = \frac{n_m(l)}{n^*(l)}$, where $\sum_{m=0}^{m=m_{max}} p_m(l) = 1$. Then, configuration entropy $H(l)$ is [33,34]:

$$H(l) = \sum_{m=0}^{m=m_{max}} p_m(l) \log(p_m(l)) \tag{11}$$

Since the underlying probability changes with the number of pixels inside the box, $H(l)$ has to be normalized so that it can be compared on different scales. The normalization factor here will be max possible value at each scale $H_{max}(l) = log(l^2 + 1)$:

$$H^*(l) = \frac{H(l)}{H_{max}(l)} \tag{12}$$

and characteristic length l_c is the scale l where $H^*(l)$ gets its maximum value, $H^*(l_c)_{max}$.

2. Software description

MULTIFRAC is an ImageJ plugin coded in JAVA that implements scaling analysis on 2D images and 3D stack images. The great advantage of this software is its ease of use, given that images to be analyzed are loaded as is usual within ImageJ graphical interface [21]. Before the analysis they can be manipulated with other plugins and functionalities implemented in ImageJ and after the analysis the results will be by default saved in sub-paths created in the original image location. In the following sections we show main components of MULTIFRAC software, their main functionalities and two illustrative examples.

2.1. Software architecture

The plugin workflow diagram is represented in Fig. 1 and it is composed of 8 main modules detailed in sub Section 2.2, three address 3D stack image analysis : *_3DFracDimBC.java*, *_3DMultifrBC.java* and *_3DMultifrGB.java*; while five address computational analysis on 2D images: *_2DFracDimBC.java*, *_2DMultifrBC.java*, *_2DMultifrGB.java*, *_2DLacunGB.java* and *_2DConfEntrCharLenGB*. There are 9 additional subroutines addressing specific tasks and analysis for main modules:

- *ColorDialog.java*: Handle dialog and options about which color will be given maximum value during calculations.
- *Linefit.java*: Minimum mean square error fit.
- *Outputpath.java*: Handles output path and folder creation for saving results.
- *Qdialog.java*: Prompt dialog for q range selection in multifractal analysis.
- *Resize.java*: Address resize or cut operations on images if necessary.
- *ToolEntrCharLen.java*: Configuration entropy and characteristic length subroutines.
- *ToolFracDim.java*: Fractal dimension subroutines.
- *ToolLacun.java*: Lacunarity analysis subroutines.
- *ToolMultifr.java*: Multifractal analysis subroutines.

2.2. Software functionalities

The main functionalities of the package are addressed by classes with explanatory names:

- **2D fractal dimension analysis**: This module implements fractal dimension computation through box counting algorithm. It admits non squared gray images, but in that case the plugin will ask the user to resize or to cut the image with included functionalities and to binarize it. Given that fractal dimension depends on the underlaying interpretation of the image, it is possible to choose which color will be counted in binary images. Then, the plugin will ask the user to restrict the calculations to some particular scales or not. Finally, it will automatically save the results and analyzed image in sub-folders where the image was loaded.
- **2D multifractal analysis box counting**: Addresses multifractal analysis with BC sliding boxes. Similar to fractal dimension analysis, the method can resize or cut the image if necessary and ask if the user want to invert the image. Additionally it includes q range selection and select minimum scale size for $\chi(q, l)$. $\chi(q, l)$, $\tau(q)$, D_q and $f(\alpha)$ representations and table results will be saved in sub-folders located in image directory.
- **2D multifractal analysis gliding box**: Includes similar functionalities than in 2D multifractal analysis box counting method, but here the resizing or cutting the image is not necessary.
- **2D Lacunarity analysis**: Compute lacunarity analysis on 2D images through gliding box sliding algorithm.
- **2D Configuration entropy and characteristic length**: Addresses configuration analysis and characteristic length.
- **3D stack fractal dimension analysis**: Includes similar functionalities as in 2D fractal dimension analysis but for 3D images.

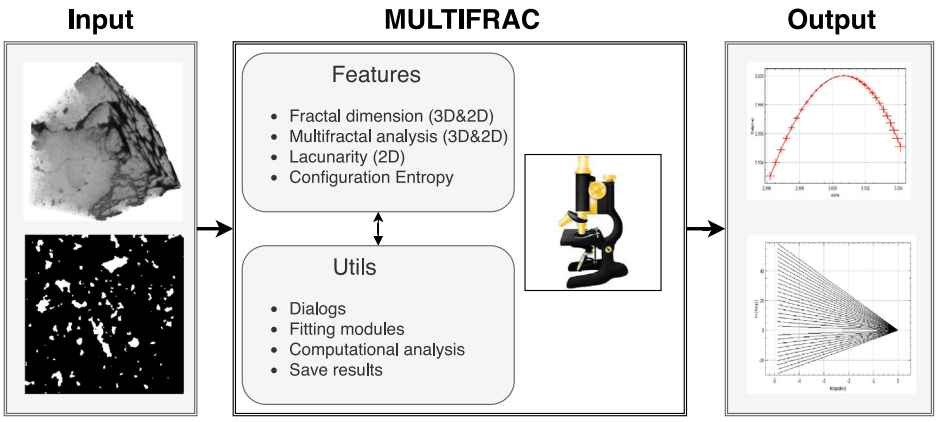

Fig. 1. Workflow diagram of MULTIFRAC.

- **3D stack multifractal analysis box counting**: Includes similar functionalities as in 2D multifractal analysis with box counting for 3D stack images.
- **3D stack multifractal analysis gliding box**: Similar functionalities as in 2D multifractal analysis with gliding box for 3D stack images.

3. Illustrative examples

The installation of MULTIFRAC is particularly user-friendly as it is integrated within ImageJ2 repositories. First, ImageJ2 or FIJI (*Fiji is Just ImageJ*) should be downloaded and started. Process to install MULTIFRAC is: (i) Run *Help|Update...* and choose *Manage update sites*, (ii) Activate *Multifrac* checkbox in the alphabetically-sorted list of update sites. Press *OK*, *Apply changes* and then (iii) Restart ImageJ or FIJI. MULTIFRAC will be integrated under the plugins menu. Updated documentation about this process, new features, functionalities and changelog can be found in ImageJ plugin webpage.

3.1. Monofractal analysis of 2D B&W Sierpinski carpet

Sierpinski carpet (Fig. 2, left) is a generalization of the Cantor set to two dimensions, resulting in a self-similar plane object with scale invariance, whose fractal dimension is analytically known. This toy model is very useful for testing the reliability and goodness of fit of methods like MULTIFRAC because of its well known properties. Its construction is recursive and starts subdividing an square into nine equal subsquares, then the one in the center is removed. This operation is recursively being applied to remaining 8 subsquares. The final result is an object with known fractal dimension of $D = \frac{log8}{log3} \approx 1.89$.

The user must first import the image to be analyzed as usual. Then MULTIFRAC will check the compatibility of the image and will suggest the requirements if they are not fulfilled. Then some boxes will prompt addressing input–output and analysis parameters, including the output folder where results will be saved – by default they will be saved in subpaths located in the original directory of the image – and scaling range of analysis. When BC is selected, but with an inadequate image size, the plugin will suggest to cut or resize the image and to check if the method is applied to black or white pixels. There is log file that records all options with a counter that says approximately how much time is left. Finally the numerical approximation of the fractal dimension of the object (Fig. 2, right) is shown and results (both images and data) are saved in the predefined path.

3.2. Multifractal analysis of 3D gray stack image

In this example we show the multifractal analysis of a 3D stack CT-scan image from a real soil sample. The CT-scan image of soil sample shows in grayscale color the three-dimensional pore structure where shades of gray represent different compositions and local radiodensities (left panel of Fig. 3). In this case, the sample is imported as a *.tif*, but any other format compatible with ImageJ is allowed, and it is even possible to load separated slides and then stack them together using ImageJ functionalities. It must be noted that computational times in multifractal analysis of 3D images and Gliding Box method quickly scales with L.

Once parameters are selected with prompted window, including q range, scales l where $\chi(q, l)$ will be fitted – one option here is to compute one time first all $\chi(q, l)$ and select appropriate scales the second time –, the output path and if we want to invert the image. The procedure is then carried out autonomously and an indicative counter of the time remaining is displayed in the log. Finally it will show multifractal features including $\chi(q, l)$ (see center panel of Fig. 3), generalized dimensions D_q, cumulant generating functions $\tau(q)$, Hölder exponents α and multifractal spectrum $f(\alpha)$ (right panel of Fig. 3), are displayed.

3.3. Additional examples

The following research papers and references therein show additional cases using this software: [12–15].

4. Impact

MULTIFRAC represents an excellent and reliable tool for researchers and engineers to understand complex structure patterns present in nature through the analysis of 2D and 3D images. The well documented algorithms and methods implemented may be applied to a broad range of fields, including analysis of CT scan images in soil science [13,14], characterization of multispectrum satellite images [35], quantification of cells morphologies in the brain [36] and defects detection in engineering applications [37]. Current available solutions for multifractal analysis are either not user-friendly or only include some basic algorithms mainly focused in 2D. This software is an invaluable tool for research groups that already use ImageJ to manipulate and analyze their images, because they just need to install this plugin from ImageJ menus to start using MULTIFRAC.

Moreover MULTIFRAC, which was initiated during 2016 is intended to be continuously developed and extended with new features. There are still algorithms that could be upgraded including different ways of box counting or to migrate some analysis

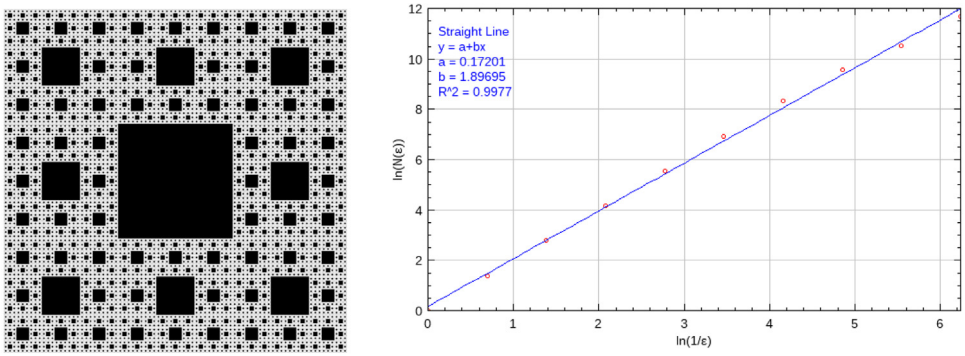

Fig. 2. Illustrative analysis of Sierpinski carpet (left) and results obtained using MULTIFRAC (right) – 1.896 – are very close to the theoretical ones — 1.892.

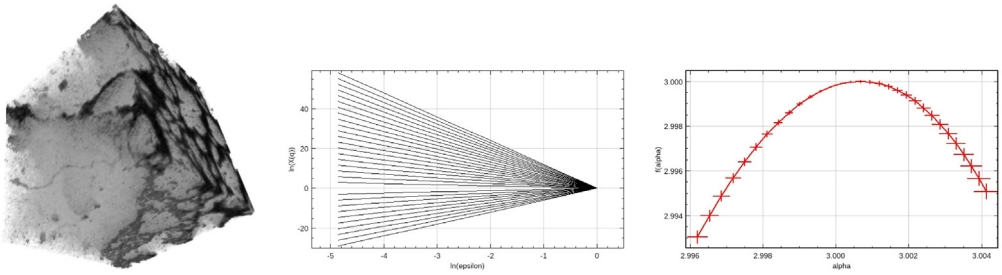

Fig. 3. Illustrative analysis of 3D stack CT scan image representing the complex structure of a soil sample (left) and some of the results obtained using MULTIFRAC including partition function $\chi(q)$ (center) and multifractal spectrum $f(\alpha)$ (right).

to 3D. MULTIFRAC is open to include new contributions and developments that address research questions in image analysis, because we firmly believe that scaling characterization and analysis of complex structures with multifractal characterization is paramount to understanding underlaying complex dynamics in many natural systems. Surely, providing software such as MULTIFRAC available to researchers will accelerate the understanding of this type of phenomenon in many different research areas.

5. Conclusions

MULTIFRAC is a user-friendly ImageJ plugin for multifractal and scaling characterization of 2D and 3D images, particularly recommended and extensively tested [12–15] in soil science research, but completely suitable to characterize images in any scientific domain. It builds on accumulated know-how during years of experience and allows the user to carry on complexity analysis over computed tomography or synthetic images in 2*D* and 3*D*. These include monofractal and multifractal analysis in 3*D* (stack) and 2*D* images, lacunarity analysis, characteristic length and configuration entropy characterization. These methods include features as partition function, cumulant generating function, generalized dimension and multifractal spectrum analysis, including several configuration options such as image redimensioning, q range selection and appropriate scale boundaries election.

MULTIFRAC aims to facilitate the application of multiscale image analysis to the scientific community through this ongoing project that will be upgraded with new features backed by trusted scientific publications.

Declaration of competing interest

The authors declare that they have no known competing financial interests or personal relationships that could have appeared to influence the work reported in this paper.

Acknowledgments

This project was supported by an NSERC Discovery Grant provided to the second author, by University of Guelph and by Project No. PGC2018-093854-B-I00 of the Spanish Ministerio de Ciencia, Innovación y Universidades of Spain.

References

[1] Rydberg J, Buckwalter KA, Caldemeyer KS, Phillips MD, Conces Jr. DJ, Aisen AM, Persohn SA, Kopecky KK. Multisection CT: scanning techniques and clinical applications. Radiographics 2000;20(6):1787–806. http://dx.doi.org/10.1148/radiographics.20.6.g00nv071787.

[2] Taina I, Heck R, Elliot T. Application of x-ray computed tomography to soil science: A literature review. Can J Soil Sci 2008;88(1):1–19. http://dx.doi.org/10.4141/CJSS06027.

[3] Olsen PA, Børresen T. Measuring differences in soil properties in soils with different cultivation practices using computer tomography. Soil Tillage Res 1997;44(1–2):1–12. http://dx.doi.org/10.1016/S0167-1987(97)00021-4.

[4] Landau LD, Lifšic EM, Lifshitz EM, Pitaevskii L. Statistical Physics: Theory of the Condensed State, Vol. 9. Butterworth-Heinemann; 1980.

[5] Castellano C, Fortunato S, Loreto V. Statistical physics of social dynamics. Rev Modern Phys 2009;81(2):591. http://dx.doi.org/10.1103/RevModPhys.81.591.

[6] Torre IG, Luque B, Lacasa L, Luque J, Hernández-Fernández A. Emergence of linguistic laws in human voice. Sci Rep 2017;7:43862. http://dx.doi.org/10.1038/srep43862.

[7] Stosic T, Stosic BD. Multifractal analysis of human retinal vessels. IEEE Trans Med Imaging 2006;25(8):1101–7. http://dx.doi.org/10.1109/TMI.2006.879316.

[8] Ji H, Yang X, Ling H, Xu Y. Wavelet domain multifractal analysis for static and dynamic texture classification. IEEE Trans Image Process 2012;22(1):286–99. http://dx.doi.org/10.1109/TIP.2012.2214040.

[9] Gerasimova E, Audit B, Roux S, Khalil A, Argoul F, Naimark O, Arneodo A. Multifractal analysis of dynamic infrared imaging of breast cancer. Europhys Lett 2014;104(6):68001. http://dx.doi.org/10.1209/0295-5075/104/68001.

[10] King RD, Brown B, Hwang M, Jeon T, George AT, Initiative ADN, et al. Fractal dimension analysis of the cortical ribbon in mild alzheimer's disease. Neuroimage 2010;53(2):471–9. http://dx.doi.org/10.1016/j.neuroimage.2010.06.050.

[11] Cheng Q. Multifractality and spatial statistics. Comput Geosci 1999;25(9):949–61. http://dx.doi.org/10.1016/S0098-3004(99)00060-6.

[12] Torre I, Martín-Sotoca JJ, Losada J, López P, Tarquis A. Scaling properties of binary and greyscale images in the context of x-ray soil tomography. Geoderma 2020;365:114205. http://dx.doi.org/10.1016/j.geoderma.2020.114205.
[13] Torre I, Losada JC, Heck R, Tarquis A. Multifractal analysis of 3D images of tillage soil. Geoderma 2018;311:167–74. http://dx.doi.org/10.1016/j.geoderma.2017.02.013.
[14] Torre IG, Losada JC, Tarquis AM. Multiscaling properties of soil images. Biosyst Eng 2018;168:133–41. http://dx.doi.org/10.1016/j.biosystemseng.2016.11.006.
[15] Tarquis AM, Torre IG, Martín-Sotoca JJ, Losada JC, Grau JB, Bird NR, Saa-Requejo A. Scaling characteristics of soil structure. In: Pedometrics. Springer; 2018, p. 155–93. http://dx.doi.org/10.1007/978-3-319-63439-5_6.
[16] Kravchenko AN, Boast CW, Bullock DG. Multifractal analysis of soil spatial variability. Agron J 1999;91(6):1033–41. http://dx.doi.org/10.2134/agronj1999.9161033x.
[17] Bird N, Díaz MC, Saa A, Tarquis AM. Fractal and multifractal analysis of pore-scale images of soil. J Hydrol 2006;322(1–4):211–9. http://dx.doi.org/10.1016/j.jhydrol.2005.02.039.
[18] Wang D, Fu B, Zhao W, Hu H, Wang Y. Multifractal characteristics of soil particle size distribution under different land-use types on the loess plateau, China. Catena 2008;72(1):29–36. http://dx.doi.org/10.1016/j.catena.2007.03.019.
[19] Karperien A. Fraclac for imagej. Charles Sturt University; 2013.
[20] Véhel JL, et al. Fraclab. 2000, www.rocq.inria.fr.fractales.
[21] Rueden CT, Schindelin J, Hiner MC, DeZonia BE, Walter AE, Arena ET, Eliceiri KW. Imagej2: Imagej for the next generation of scientific image data. BMC Bioinformatics 2017;18(1):529. http://dx.doi.org/10.1186/s12859-017-1934-z.
[22] Mandelbrot BB. The Fractal Geometry of Nature. WH Freeman New York; 1982.
[23] Mandelbrot B. How long is the coast of britain? Statistical self-similarity and fractional dimension. Science 1967;156(3775):636–8. http://dx.doi.org/10.1126/science.156.3775.636.
[24] Ching D, Taylor GJ, Mouginis-Mark P, Bruno BC. Fractal dimensions of rampart impact craters on mars. In: Lunar and Planetary Science Conference, Vol. 24. 1993.
[25] Saa A, Gascó G, Grau JB, Antón JM, Tarquis AM. Comparison of gliding box and box-counting methods in river network analysis. Nonlinear Process Geophys 2007;14(5):603–13. http://dx.doi.org/10.5194/npg-14-603-2007.
[26] Park Y, Lee K, Ziegler TR, Martin GS, Hebbar G, Vidakovic B, Jones DP. Multifractal analysis for nutritional assessment. PLoS One 2013;8(8). http://dx.doi.org/10.1371/journal.pone.0069000.
[27] Halsey TC, Jensen MH, Kadanoff LP, Procaccia I, Shraiman BI. Fractal measures and their singularities: The characterization of strange sets. Phys Rev A 1986;33(2):1141. http://dx.doi.org/10.1016/0920-5632(87)90036-3.
[28] Mandelbrot BB. Multifractal measures, especially for the geophysicist. In: Fractals in Geophysics. Springer; 1989, p. 5–42. http://dx.doi.org/10.1007/BF00874478.
[29] Millán H, Cumbrera R, Tarquis AM. Multifractal and levy-stable statistics of soil surface moisture distribution derived from 2d image analysis. Appl Math Model 2016;40(3):2384–95. http://dx.doi.org/10.1016/j.apm.2015.09.063.
[30] Salat H, Murcio R, Arcaute E. Multifractal methodology. Physica A 2017;473:467–87. http://dx.doi.org/10.1016/j.physa.2017.01.041.
[31] Plotnick RE, Gardner RH, O'Neill RV. Lacunarity indices as measures of landscape texture. Landsc Ecol 1993;8(3):201–11. http://dx.doi.org/10.1007/BF00125351.
[32] Gefen Y, Meir Y, Mandelbrot BB, Aharony A. Geometric implementation of hypercubic lattices with noninteger dimensionality by use of low lacunarity fractal lattices. Phys Rev Lett 1983;50(3):145. http://dx.doi.org/10.1103/PhysRevLett.50.145.
[33] Allain C, Cloitre M. Characterizing the lacunarity of random and deterministic fractal sets. Phys Rev A 1991;44(6):3552. http://dx.doi.org/10.1103/physreva.44.3552.
[34] Andraud C, Beghdadi A, Haslund E, Hilfer R, Lafait J, Virgin B. Local entropy characterization of correlated random microstructures. Physica A 1997;235(3–4):307–18. http://dx.doi.org/10.1016/S0378-4371(96)00354-8.
[35] Alonso C, Tarquis AM, Zúñiga I, Benito RM. Spatial and radiometric characterization of multi-spectrum satellite images through multi-fractal analysis. Nonlinear Process Geophys 2017;24(2). http://dx.doi.org/10.5194/npg-24-141-2017.
[36] Kalmanti E, Maris TG. Fractal dimension as an index of brain cortical changes throughout life. Vivo 2007;21(4):641–6.
[37] Yao B, Imani F, Sakpal AS, Reutzel EW, Yang H. Multifractal analysis of image profiles for the characterization and detection of defects in additive manufacturing. J Manuf Sci Eng 2018;140(3). http://dx.doi.org/10.1115/1.4037891.